Prospects for observing the missing $2D$ and $1F$ charmonium states around 4 GeV

刘成郗

兰州大学

合作者：满自龙，高天乐，刘翔

2026.3.30

第五届强子与重味物理理论与实验联合研讨会

C.X.Liu, Z.L.Man, T.L.Gao and X.Liu, arXiv:2411.15689(2026)

Outline

1. Background
2. The $2D$ and $1F$ charmonia
3. Production of charmonium
4. Summary

蘭州大學

Background

Charmonium spectrum

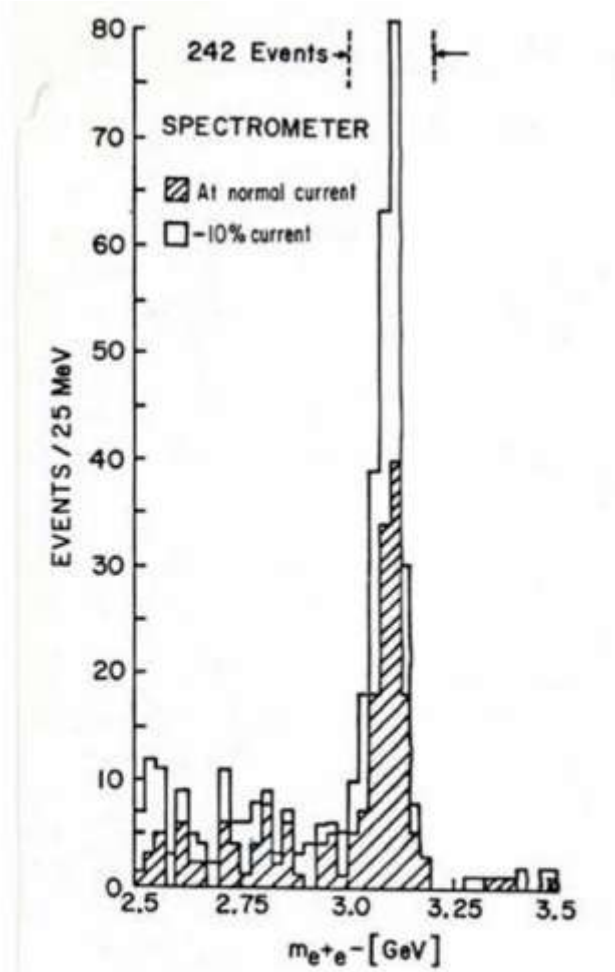

Fig. 1 The J-ψ signal detected by Ting and his group at BNL. The J-ψ appears as a quite striking peak in the distribution of the total mass of the electron-positron pairs.

2024 marks the 50th anniversary of the discovery of the J/ψ particle, the first charmonium state. Since then, over a dozen charmonium states have been identified

6^1S_0	6^3S_1	6^1P_1	6^3P_0 $\chi_{c0}(4700)$ 4694^{+16}_{-5} 87^{+28}_{-14}	6^3P_1 $\chi_{c1}(4685)$ 4684 ± 15 130 ± 40	6^3P_2	6^3D_1
5^1S_0	5^3S_1 $\psi(4415)$ 4415 ± 5 110 ± 22	5^1P_1	5^3P_0 $\chi_{c0}(4500)$ 4474 ± 4 77 ± 10	5^3P_1	5^3P_2	5^3D_1 $\psi(4660)$ 4641 ± 10 73 ± 11
4^1S_0	4^3S_1 $\psi(4230)$ 4222 ± 2.3 49 ± 7	4^1P_1	4^3P_0	4^3P_1 $\chi_{c1}(4274)$ 4286 ± 8.0 51 ± 7	4^3P_2	4^3D_1 $\psi(4500)$ 4469 ± 26 246 ± 36
3^1S_0	3^3S_1 $\psi(4040)$ 4040 ± 4 84 ± 12	3^1P_1	3^3P_0	3^3P_1 $\chi_{c1}(4140)$ 4146 ± 3.0 19^{+7}_{-5}	3^3P_2	3^3D_1 $\psi(4360)$ 4374 ± 7 118 ± 12
2^1S_0 $\eta_c(2S)$ 3637 ± 0.9 11.8 ± 1.6	2^3S_1 $\psi(2S)$ 3686 ± 0.011 0.293 ± 0.009	2^1P_1	2^3P_0 $\chi_{c0}(3915)$ 3922 ± 0.18 20 ± 4	2^3P_1 $\chi_{c1}(3872)$ 3871 ± 0.06 1.19 ± 0.21	2^3P_2 $\chi_{c2}(3930)$ 3922 ± 1.0 35.2 ± 2.2	2^3D_1 $\psi(4160)$ 4191 ± 5 69 ± 10
1^1S_0 η_c 2984 ± 0.4 30.5 ± 0.5	1^3S_1 J/ψ 3096 ± 0.006 0.093 ± 0.002	1^1P_1 $h_c(1P)$ 3525 ± 0.14 0.78 ± 0.28	1^3P_0 $\chi_{c0}(1P)$ 3414 ± 0.3 10.7 ± 0.6	1^3P_1 $\chi_{c1}(1P)$ 3510 ± 0.05 0.84 ± 0.04	1^3P_2 $\chi_{c2}(1P)$ 3556 ± 0.07 1.98 ± 0.09	1^3D_1 $\psi(3770)$ 3773 ± 0.7 27.2 ± 1.0
0^{-+}	1^{--}	1^{+-}	0^{++}	1^{++}	2^{++}	1^{--}

3^3D_2	3^3D_3	3^1D_2	3^1F_3	3^3F_2	3^3F_3	3^3F_4	3^1G_4	3^3G_3	3^3G_4	3^3G_5
2^3D_2	2^3D_3	2^1D_2	2^1F_3	2^3F_2	2^3F_3	2^3F_4	2^1G_4	2^3G_3	2^3G_4	2^3G_5
1^3D_2 $\psi_2(3823)$ 3823 ± 0.34 < 2.9	1^3D_3 $\psi_3(3842)$ 3842 ± 0.2 2.8 ± 0.6	1^1D_2	1^1F_3	1^3F_2	1^3F_3	1^3F_4	1^1G_4	1^3G_3	1^3G_4	1^3G_5
2^{--}	3^{--}	2^{-+}	3^{+-}	2^{++}	3^{++}	4^{++}	4^{-+}	3^{--}	4^{--}	5^{--}

Quantum number $(n^{2S+1}L_J)$	Candidate states
State	Established states
Mass (MeV)	Our focused states
Width (MeV)	Missing states

However, the charmonium family is still not yet fully established, especially for those high-lying states

From quenched to unquenched models

The discovery since 2003 of charmonium-like XYZ states challenged quenched models, making unquenched models essential for constructing the higher charmonium spectrum.

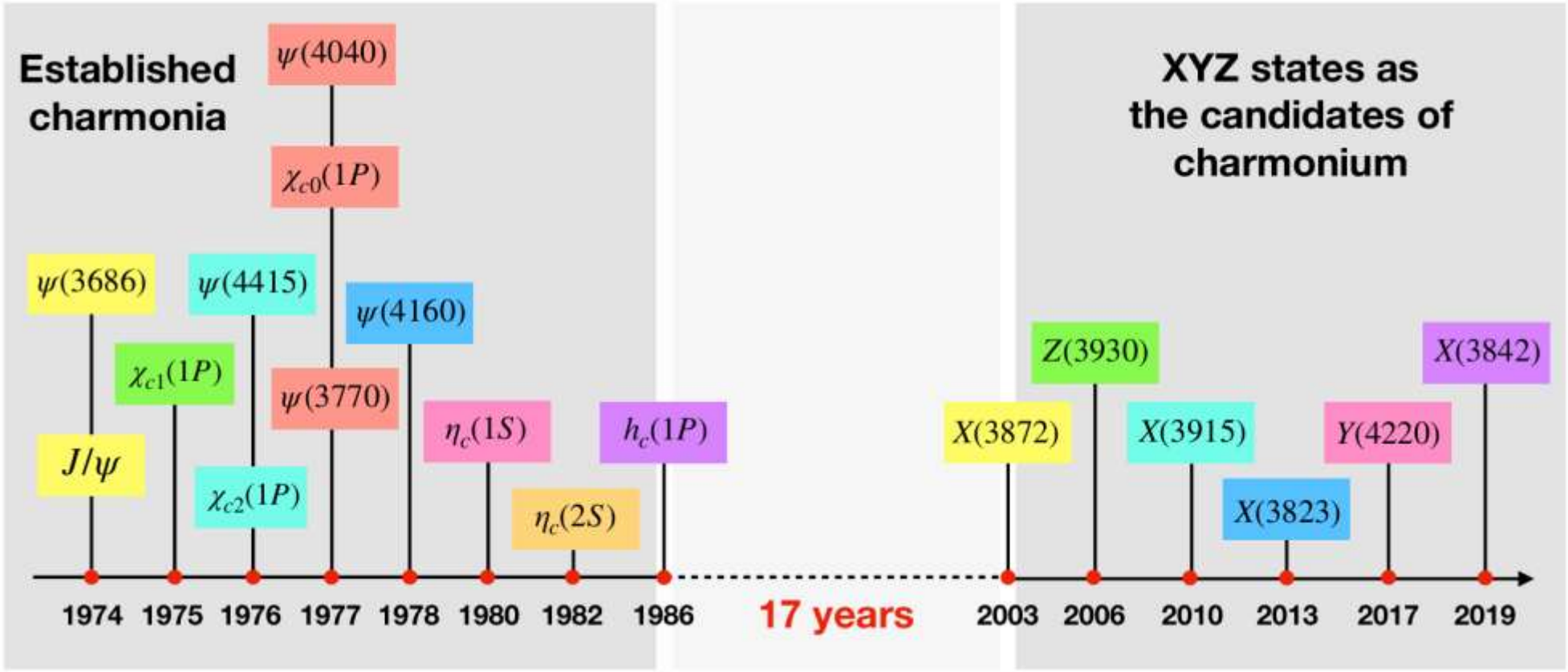

Charmonium discovery → Quenched model

New hadron states → Quenched model outpaced

Unquenched charmonium spectrum

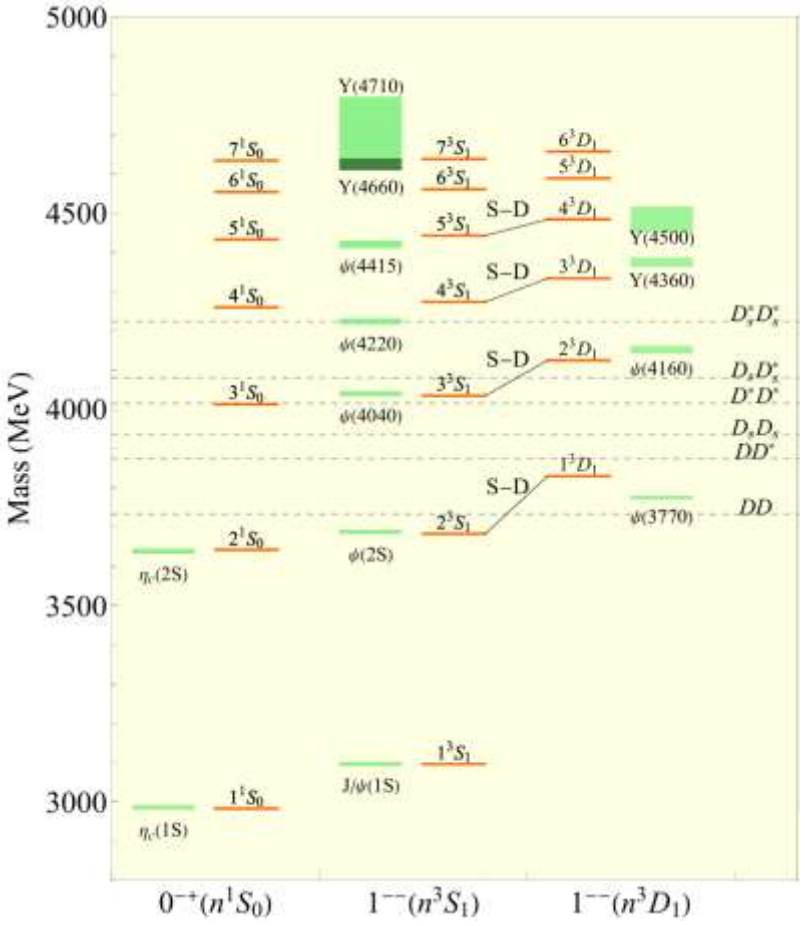

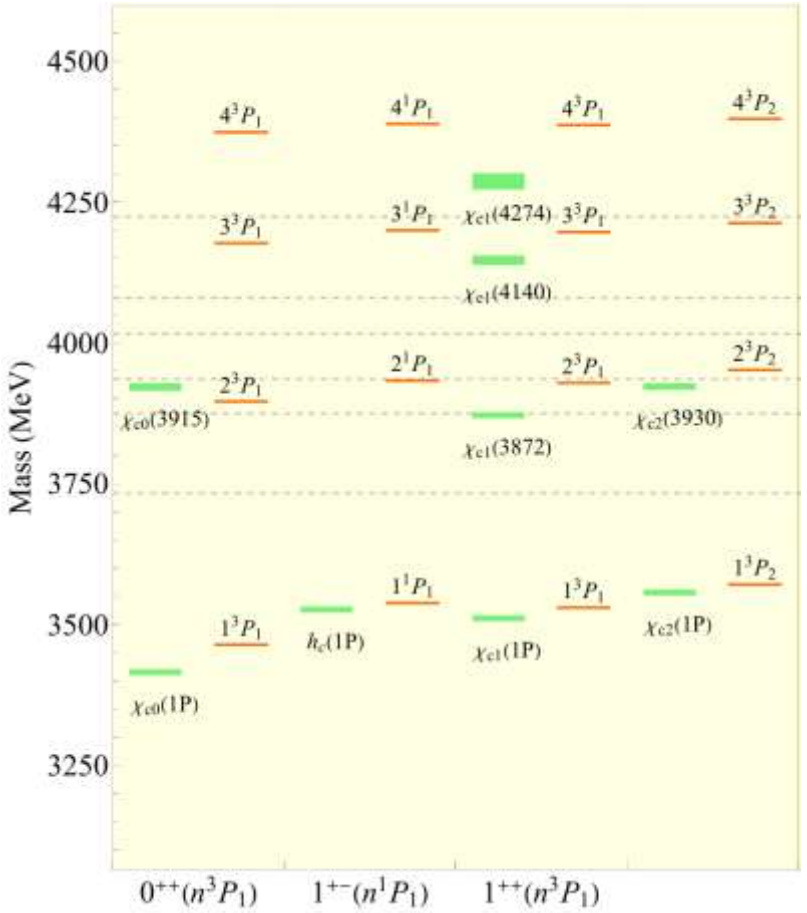

Unquenched effects are essential for describing higher radial and orbital excitations

Currently, the understanding of high-lying charmonium remains relatively limited

Therefore, it is time to extend our study and predict the higher radial and orbital charmonium spectrum

The $2D$ and $1F$ charmonia

The Godfrey-Isgur (GI) model

In the nonrelativistic limit, the effective potential has a familiar format:

$$\tilde{H} = (p^2 + m_1^2)^{1/2} + (p^2 + m_2^2)^{1/2} + \tilde{V}_{\text{eff}}(\boldsymbol{p}, \boldsymbol{r}),$$

$$V_{\text{eff}}(r) = H^{\text{conf}} + H^{\text{hyp}} + H^{\text{so}},$$

$$H^{\text{conf}} = br - \frac{4\alpha_s(r)}{3r} + c$$

↑ Cornell potential

$$H^{\text{hyp}} = \frac{4\alpha_s(r)}{3m_1 m_2}\left[\frac{8\pi}{3}\boldsymbol{S}_1 \cdot \boldsymbol{S}_2 \delta^3(\boldsymbol{r}) + \frac{1}{r^3}\left(\frac{3(\boldsymbol{S}_1 \cdot \boldsymbol{r})(\boldsymbol{S}_2 \cdot \boldsymbol{r})}{r^2} - \boldsymbol{S}_1 \cdot \boldsymbol{S}_2\right)\right],$$

$$H^{\text{so}} = H^{\text{so(cm)}} + H^{\text{so(tp)}}.$$

$$H^{\text{so(cm)}} = \frac{4\alpha_s(r)}{3r^3}\left(\frac{\boldsymbol{S}_1}{m_1^2} + \frac{\boldsymbol{S}_2}{m_2^2} + \frac{\boldsymbol{S}_1 + \boldsymbol{S}_2}{m_1 m_2}\right) \cdot \boldsymbol{L},$$

$$H^{\text{so(tp)}} = -\frac{1}{2r}\frac{\partial H^{\text{scr}}}{\partial r}\left(\frac{\boldsymbol{S}_1}{m_1^2} + \frac{\boldsymbol{S}_2}{m_2^2}\right) \cdot \boldsymbol{L},$$

To account for relativistic effects, two modifications are introduced. First, a smearing function is applied:

$$\tilde{V}(r) = \int d^3\boldsymbol{r}' \rho(\boldsymbol{r} - \boldsymbol{r}') V(r'), \quad \rho(\boldsymbol{r} - \boldsymbol{r}') = \frac{\sigma^3}{\pi^{3/2}} \exp\left[-\sigma^2(\boldsymbol{r} - \boldsymbol{r}')^2\right]$$

Second, to account for the center of mass effects, momentum-dependent factors are introduced:

$$\tilde{G}(r) \to \left(1 + \frac{p^2}{E_1 E_2}\right)^{1/2} \tilde{G}(r) \left(1 + \frac{p^2}{E_1 E_2}\right)^{1/2},$$

$$\tilde{V}_i(r) \to \left(\frac{m_1 m_2}{E_1 E_2}\right)^{1/2+\epsilon_i} \tilde{V}_i(r) \left(\frac{m_1 m_2}{E_1 E_2}\right)^{1/2+\epsilon_i}.$$

Finally, the screening effect is introduced to account for the unquenched effect, it is common to replace the line potential with the screening potential

$$br \to \frac{b(1 - e^{-\mu r})}{\mu}, \quad H^{\text{scr}} = \frac{b(1 - e^{-\mu r})}{\mu} - \frac{4\alpha_s(r)}{3r} + c.$$

The Quark-Pair-Creation model

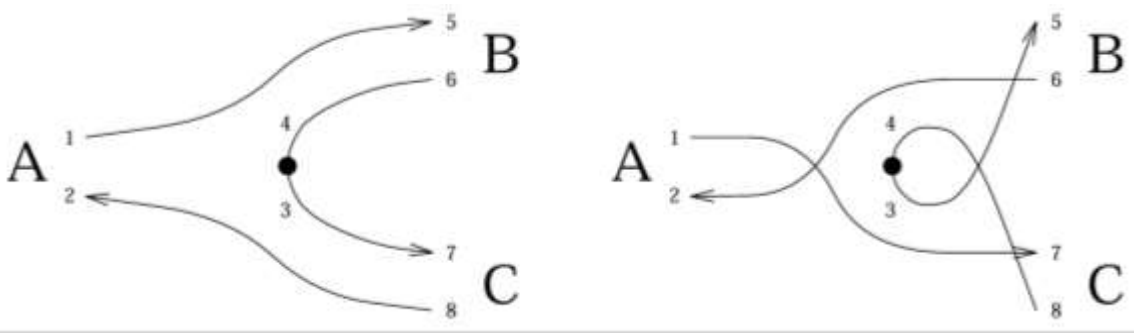

A two-body OZI-allowed decay process $A \to BC$ can be expressed as

$$\langle BC|\mathcal{T}|A\rangle = \delta^3(\mathbf{P}_B + \mathbf{P}_C)\mathcal{M}^{M_{J_A}M_{J_B}M_{J_C}},$$

$$\mathcal{T} = -3\gamma \sum_{m,i,j} \langle 1m; 1-m \mid 00\rangle \int d\boldsymbol{p}_3 d\boldsymbol{p}_4 \delta^3(\boldsymbol{p}_3 + \boldsymbol{p}_4) \times \mathcal{Y}_{1m}\left(\frac{\boldsymbol{p}_3 - \boldsymbol{p}_4}{2}\right)\chi^{34}_{1,-m}\phi^{34}_0\left(\omega^{34}_0\right)_{ij} b^\dagger_{3i}(\boldsymbol{p}_3)\, b^\dagger_{4j}(\boldsymbol{p}_4),$$

The states $|A\rangle$, $|B\rangle$, and $|C\rangle$ refer to the mock states associated with mesons A, B, and C.

By applying the Jacobi-Wick formula, the strong decay partial width for a given decay mode of $A \to BC$ reads as

$$\mathcal{M}^{JL}(A \to BC) = \frac{\sqrt{4\pi(2L+1)}}{2J_A+1} \sum_{M_{J_B}M_{J_C}} \langle L0; JM_{J_A}|J_A M_{J_A}\rangle \times \langle J_B M_{J_B}; J_C M_{J_C}|J_A M_{J_A}\rangle \times \mathcal{M}^{M_{J_A}M_{J_B}M_{J_C}}(\boldsymbol{P}),$$

$$\Gamma_{A\to BC} = \frac{\pi^2}{4}\frac{|\boldsymbol{P}|}{m_A^2} \sum_{J,L} |\mathcal{M}^{JL}(\boldsymbol{P})|^2,$$

The QPC model primarily dependences on the hadron wave functions and the γ parameter.

Here we use $\gamma = 5.84$ and expand the wave functions obtained from GI model with the simple harmonic oscillator (SHO) wave function

$$\phi^p_{nlm}(R, \mathbf{p}) = R^p_{nl}(R, p)Y_{lm}(\hat{\mathbf{p}}),$$

$$R^p_{nl}(R, p) = (-1)^n(-\mathrm{i})^l R^{\frac{3}{2}+l}\sqrt{\frac{2n!}{\Gamma(n+l+\frac{3}{2})}} L_n^{l+\frac{1}{2}}(R^2p^2)\mathrm{e}^{-\frac{R^2p^2}{2}} p^l.$$

Radiative decay

The quark-photon electromagnetic coupling is described by

$$H_e = -\sum_j e_j \bar{\psi}_j \gamma_\mu^j A^\mu(\mathbf{k}, \mathbf{r}) \psi_j,$$

The nonrelativistic expansion of H_e can be written as

$$h_e \simeq \sum_j \left[e_j \mathbf{r}_j \cdot \boldsymbol{\epsilon} - \frac{e_j}{2m_j} \boldsymbol{\sigma}_j \cdot (\boldsymbol{\epsilon} \times \hat{\mathbf{k}}) \right] e^{-i\mathbf{k}\cdot\mathbf{r}_j},$$

The standard helicity transition amplitude $\mathcal{A}_\lambda$ between the initial state $|J_i \lambda_i\rangle$ and the final state $\langle J_f \lambda_f|$ is given by

$$\mathcal{A}_\lambda = -i \sqrt{\frac{\omega_\gamma}{2}} \left\langle J_f \lambda_f \left| h_e \right| J_i \lambda_i \right\rangle,$$

Finally, the partial decay widths for the electromagnetic transitions are given by

$$\Gamma = \frac{|\mathbf{k}|^2}{\pi} \frac{2}{2J_i + 1} \frac{M_f}{M_i} \sum_\lambda |\mathcal{A}_\lambda|^2,$$

We can use the multipole expansion to separate the electric and magnetic transition parts as

Process	Multipole contribution
$n^3S_1 \leftrightarrow m^1S_0$	M1
$n^3P_J \leftrightarrow m^3S_1$	E1, M2
$n^1P_1 \leftrightarrow m^1S_0$	E1
$n^3D_J \leftrightarrow m^3P_J$	E1, E3, M2, M4
$n^1D_1 \leftrightarrow m^1P_1$	E1, E3
$n^3P_J \leftrightarrow m^1P_1$	M1, M3

Phys. Rev. D 95, 034026 (2017)

Generally the E1 channel is the primary channel of electromagnetic transitions.

The masses of D- and F-wave charmonia

- The masses of the missing $2D$ states exhibit near degeneracy at approximately 4140 MeV
- The masses of the $1F$ states exhibit near degeneracy at approximately 4070MeV
- The masses of $1F$ states are close to the $D^*\bar{D}^*$ threshold.
- In such cases, the inclusion of state mixing may increase the final masses.

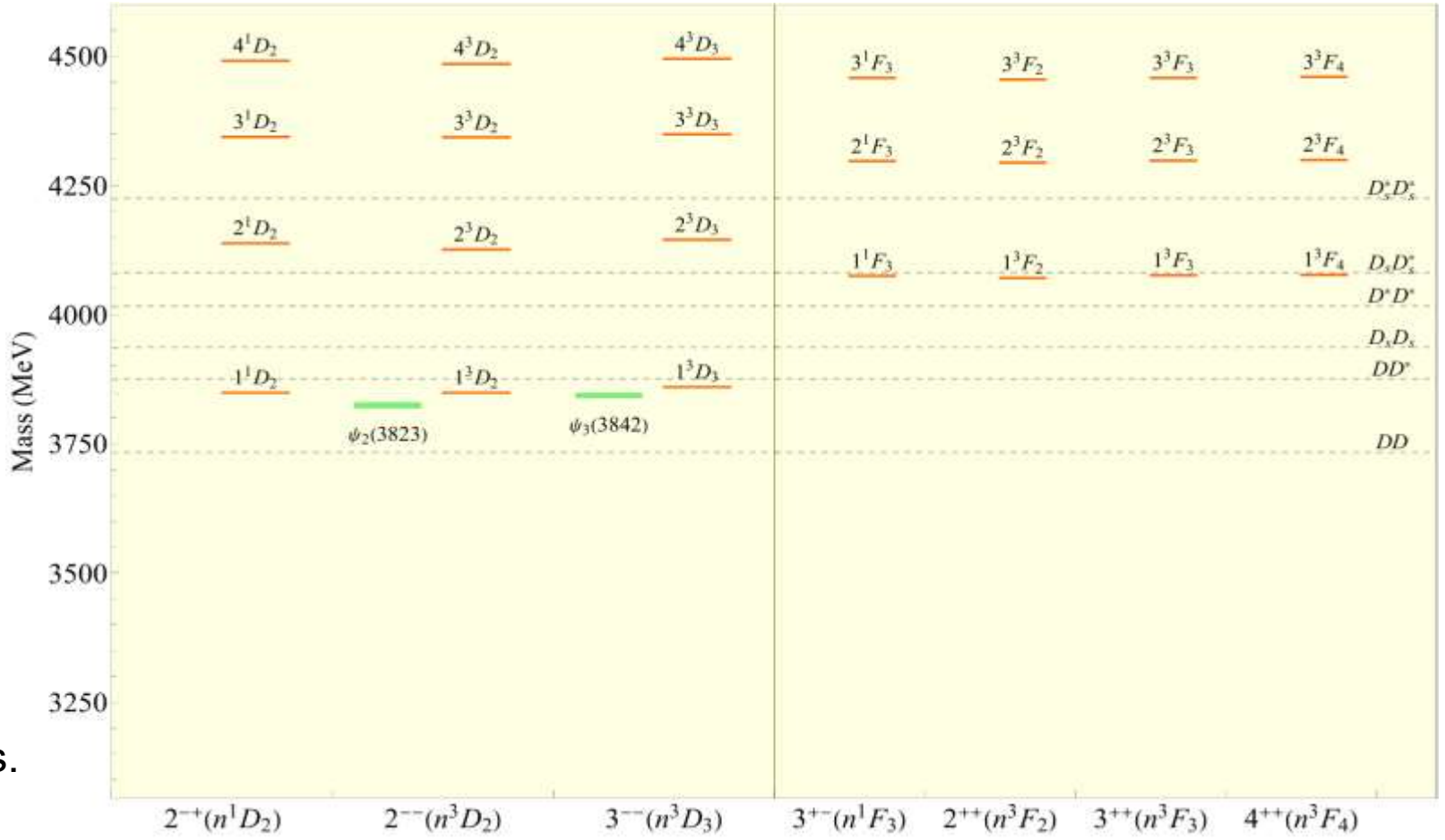

The decay behaviors of D- and F-wave charmonia

	2^1D_2		2^3D_2		2^3D_3	
Mass	4137		4137		4144	
Strong decay						
Mode	Γ_{thy} (MeV)	Br	Γ_{thy} (MeV)	Br	Γ_{thy} (MeV)	Br
$D\bar{D}$	✗		✗		$3.3^{+0.7}_{-0.5}$	6.0%
$D\bar{D}^*$[a]	$29.5^{+5.0}_{-5.0}$	51.0%	$22.9^{+3.8}_{-4.0}$	47.1%	$21.8^{+3.8}_{-3.6}$	40.1%
$D^*\bar{D}^*$	$27.2^{+4.6}_{-4.7}$	47.0%	$24.0^{+4.8}_{-3.6}$	49.3%	$28.8^{+3.8}_{-5.7}$	53.0%
$D_s\bar{D}_s$	✗		✗		$0.4^{+0.02}_{-0.1}$	0.7%
$D_s\bar{D}_s^*$	$1.2^{+0.2}_{-0.2}$	2.0%	$1.8^{+0.4}_{-0.3}$	3.6%	$0.1^{+0.01}_{-0.03}$	0.2%
Total	$57.9^{+9.8}_{-9.9}$	100%	$48.7^{+9.0}_{-7.9}$	100%	$54.4^{+8.3}_{-9.9}$	100%
Radiative decay						
	Mode	Γ_{thy} (keV)	Mode	Γ_{thy} (keV)	Mode	Γ_{thy} (keV)
	$2^1P_1\gamma$	167	$2^3P_1\gamma$	128	$2^3P_2\gamma$	213
	$1^1P_1\gamma$	58.45	$2^3P_2\gamma$	63	$1^3P_2\gamma$	41

	1^1F_3		1^3F_2		1^3F_3		1^3F_4	
Mass	4074		4070		4075		4076	
Strong decay								
Mode	Γ_{thy} (MeV)	Br	Γ_{thy} (MeV)	Br	Γ_{thy} (MeV)	Br	Γ_{thy} (MeV)	Br
$D\bar{D}$	✗		$50.5^{+8.9}_{-8.4}$	44.9%	✗		$8.1^{+1.1}_{-1.6}$	21.3%
$D\bar{D}^*$	$67.8^{+11.5}_{-11.6}$	86.1%	$56.4^{+9.5}_{-9.6}$	50.1 %	$87.6^{+15.0}_{-14.9}$	92.0%	$5.9^{+0.9}_{-1.1}$	15.5%
$D^*\bar{D}^*$	$11.0^{+3.2}_{-0.9}$	13.9%	$3.4^{+1.1}_{-0.2}$	3.1%	$7.6^{+2.3}_{-0.6}$	8.00%	$23.9^{+7.0}_{-1.9}$	62.9%
$D_s\bar{D}_s$	✗		$2.2^{+0.1}_{-0.7}$	1.9%	✗		$0.1^{+0.07}_{-0.08}$	0.3%
total	$78.8^{+14.7}_{-12.5}$	100%	$112.5^{+19.6}_{-19.0}$	100%	$95.2^{+17.3}_{-15.4}$	100%	$38.0^{+9.0}_{-4.6}$	100%
Radiative decay								
	Mode	Γ_{thy} (keV)	Mode	Γ_{thy} (keV)	Mode	Γ_{thy} (keV)	Mode	Γ_{thy} (keV)
	$1^1D_2\gamma$	249	$1^3D_1\gamma$	440	$1^3D_2\gamma$	295	$1^3D_3\gamma$	269

- For the $2D$ states, the dominant hadronic decays are $D\bar{D}^*$ and $D^*\bar{D}^*$
- For the $1F$ states, the $D\bar{D}$ channel is also a dominant decay channel.
- The dominant radiative decay $E1$ processes exhibit branching ratios on the order of 0.1%

The $X(4160)$ as a candidate of $\eta_{c2}(2D)$ state

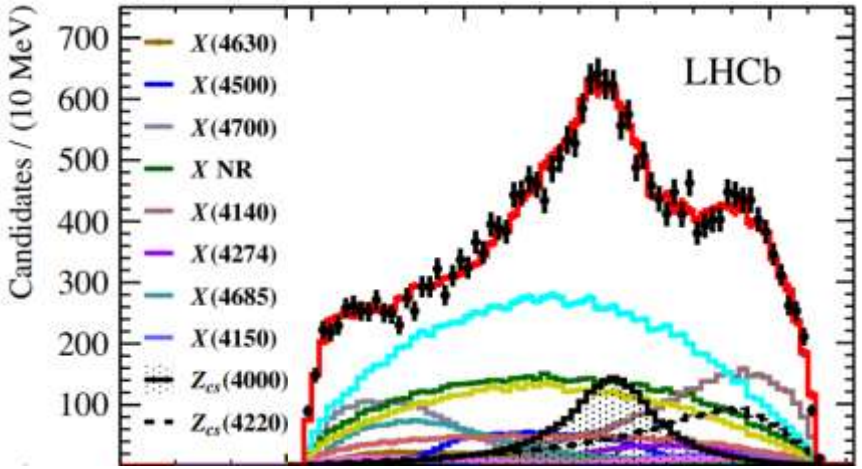

Phys. Rev. Lett. 127, 082001 (2021)

The mass dependence

We presented the decay behaviors of these states near $D^*\bar{D}^*$ open flavor threshold

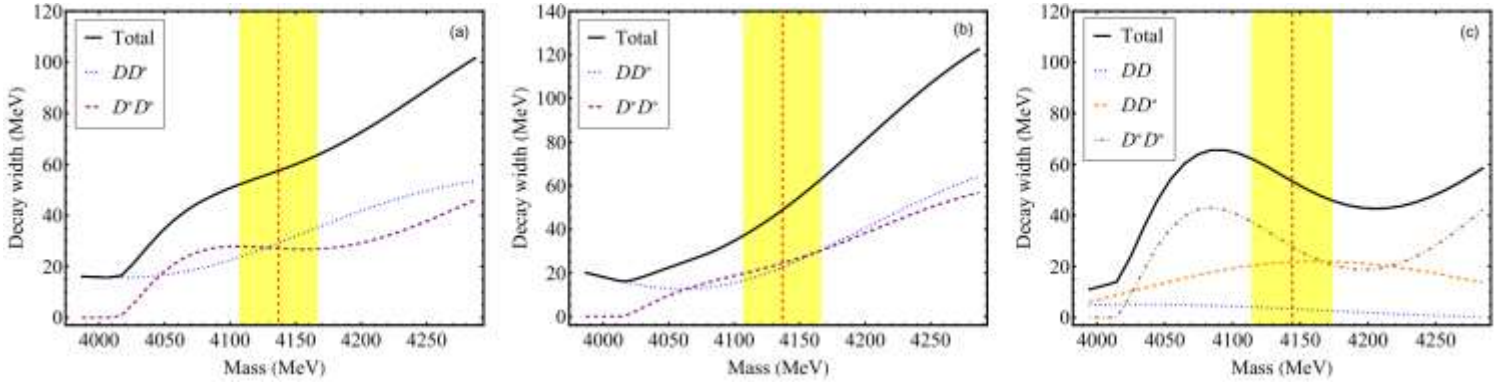

Figures (a), (b), and (c) display the partial widths of $\eta_{c2}(4137)$, $\psi_2(4137)$, and $\psi_3(4144)$ states

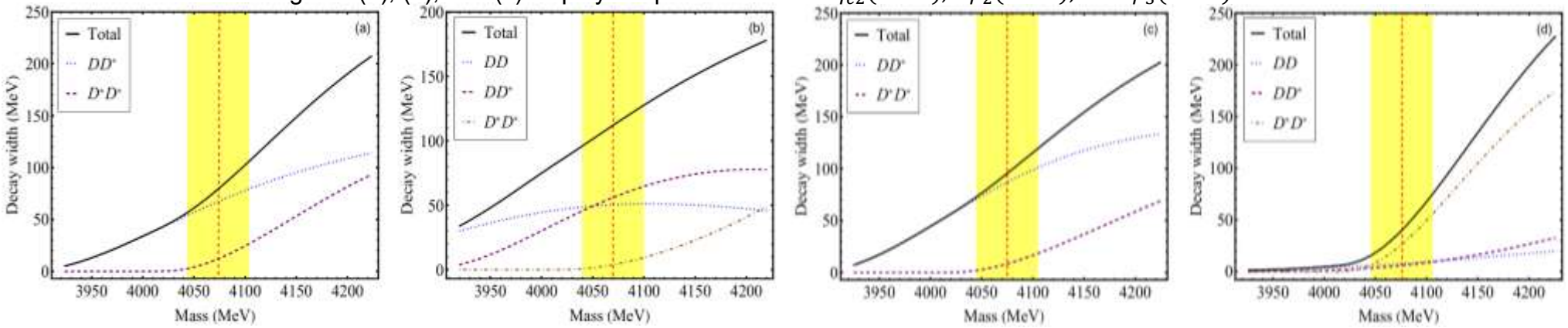

Figures (a), (b), (c), and (d) display the partial widths as a function of mass for the $h_{c3}(4074)$, $\chi_{c2}(4070)$, $\chi_{c3}(4075)$ and $\chi_{c4}(4076)$ states

Their decay properties exhibit a strong dependence on the precise mass values, especially for $1F$ states. This is most evident for the 1^3F_4 state

Therefore, precise experimental determination of their masses is crucial

Production of charmonium

Production through e^+e^- collisions

The e^+e^- annihilation process is a primary mechanism for producing charmonium states

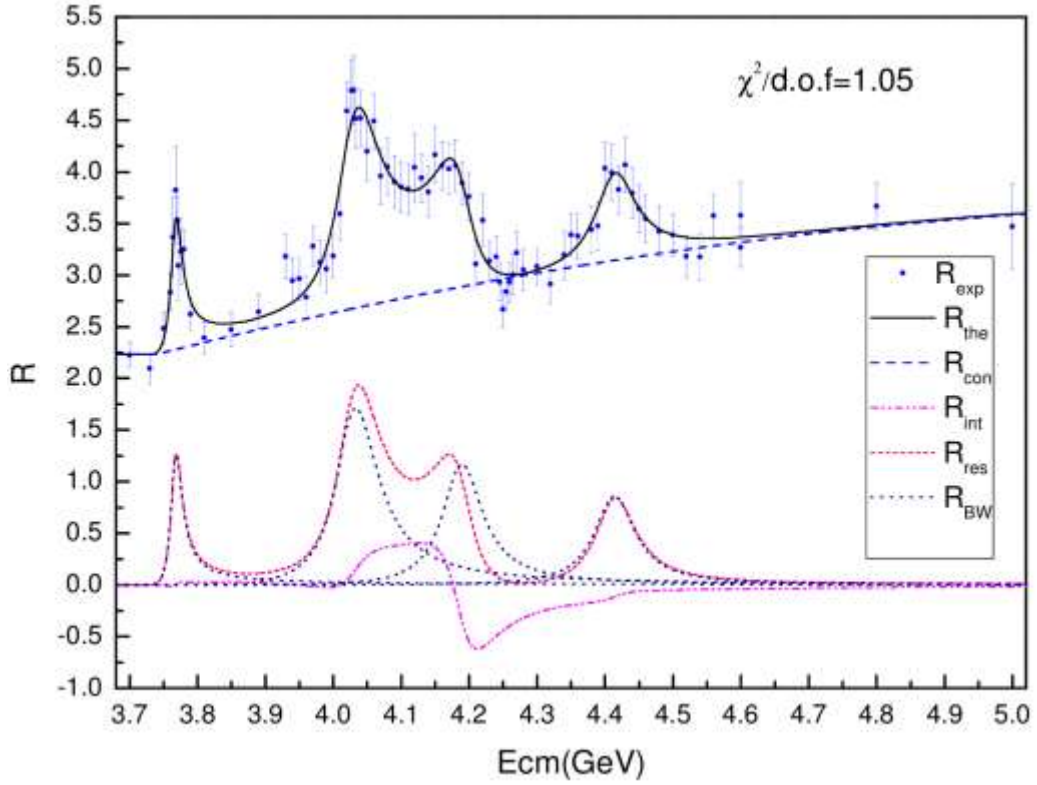

Physics Letters B 660 315–319 (2008)

For example, among the $2D$ states, the $\psi(4160)$ is predominantly observed in e^+e^- collisions

Possible production processes of $2D$ and $1F$ states

states	mode	process	J^{PC}							m_ψ (GeV)
			2^{--}	3^{--}	2^{-+}	2^{++}	3^{++}	4^{++}	3^{+-}	
$2D$	radiative decay	$\gamma\eta_c(2^1D_2)$	–	–	P	–	–	–	–	> 4.2
	hidden-charm decay	$\pi^+\pi^-\psi(2^3D_J)$	D	D	–	–	–	–	–	> 4.66
		$\eta\psi(2^3D_J)$	P	F	–	–	–	–	–	> 4.71
		$\omega\eta_c(2^1D_2)$	-	-	P	–	–	–	–	> 4.94
$1F$	radiative decay	$\gamma\chi_c(1^3F_J)$	–	–	–	S	D	D	–	> 4.1
	hidden-charm decay	$\omega\chi_c(1^3F_J)$	–	–	–	S	D	D	–	> 4.85
		$\eta\chi_c(1^1F_J)$	–	–	–	D	–	–	D	> 4.62

The BESIII experiment has accumulated substantial data around 4.2 GeV, while data at higher energies ($\sqrt{s} \geq 4.4$ GeV) are less abundant.

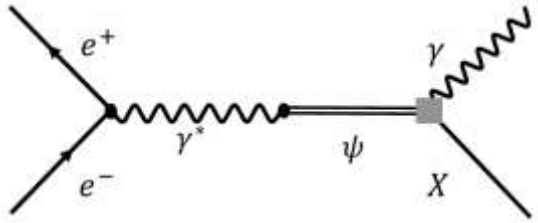

Radiative decay processes of $\psi(4230)$

Hadronic loop mechanism

To account for the sizable coupled-channel effects in high-lying states, we adopt the hadronic loop mechanism for production estimates.

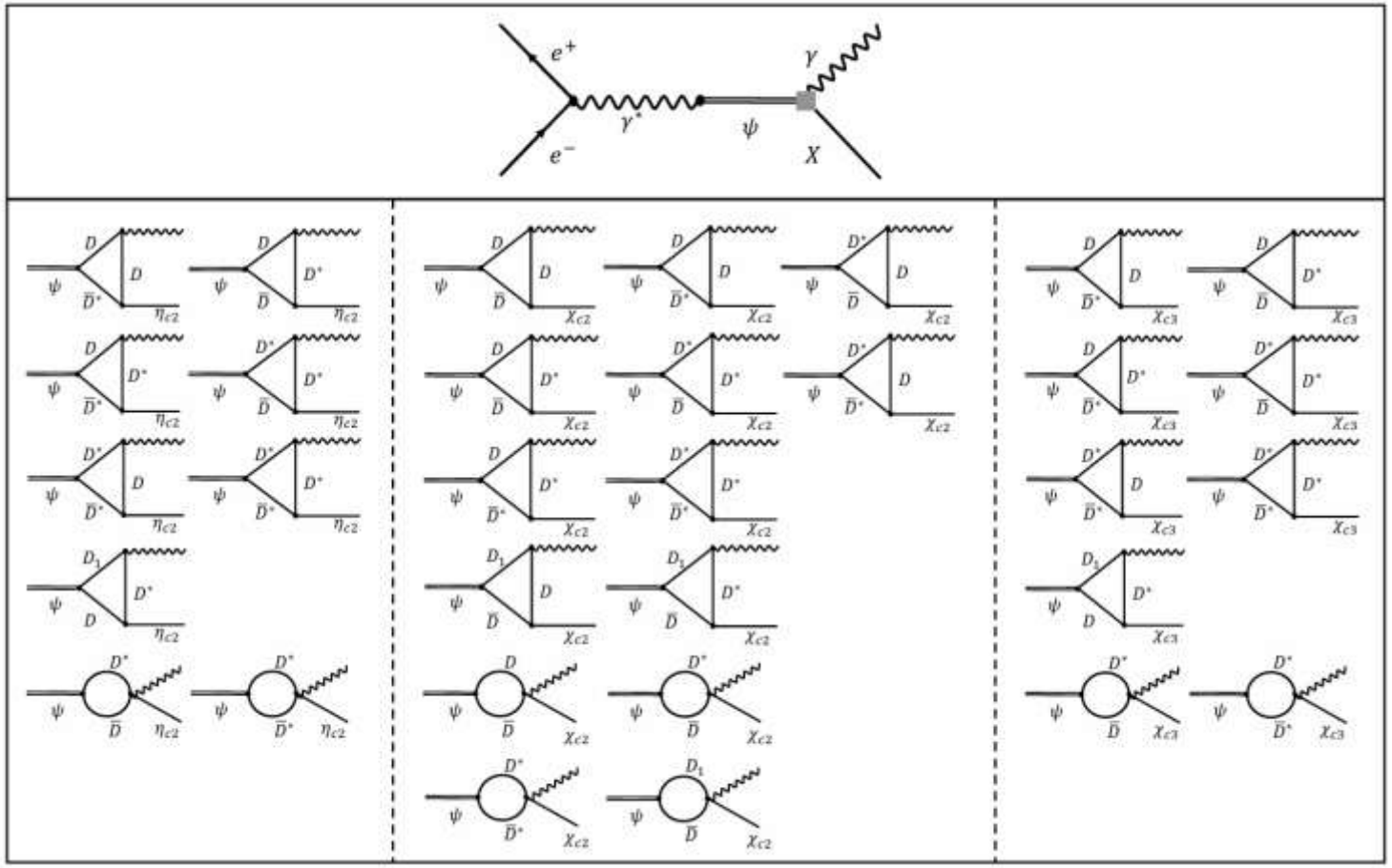

$$\mathcal{M} = \int \frac{d^4q}{(2\pi)^4} \frac{\mathcal{V}_1\mathcal{V}_2\mathcal{V}_3}{\mathcal{D}_1\mathcal{D}_2\mathcal{D}_E}\mathcal{F}^2(q^2),$$

$$\mathcal{F}(q^2) = \left(\frac{m_E^2 - \Lambda^2}{q^2 - \Lambda^2}\right)^2, \quad \Lambda = m_E + \alpha\Lambda_{QCD},$$

$$\mathcal{L}_S = i\, g_S \mathrm{Tr}[S_{Q\bar{Q}} \bar{H}^{\bar{Q}q} \gamma^\mu \overleftrightarrow{\partial}_\mu \bar{H}^{Q\bar{q}}],$$

$$\mathcal{L}_D = i\, g_D \mathrm{Tr}[D^{\mu\nu}_{Q\bar{Q}} \bar{H}^{\bar{Q}q} \overleftrightarrow{\partial}_\mu \gamma_\nu \bar{H}^{Q\bar{q}}].$$

$$\mathcal{L}_F = g_F \mathrm{Tr}[F^{\mu\nu\theta}_{Q\bar{Q}} \bar{H}^{\bar{Q}q} \overleftrightarrow{\partial}_\mu \overleftrightarrow{\partial}_\theta \gamma_\nu \bar{H}^{Q\bar{q}}].$$

Gauge invariance:

$$\mathcal{M}^{\mathrm{Tot}} = \epsilon^\mu_\gamma \mathcal{M}^{\mathrm{Tot}}_\mu, \quad \mathcal{M}^\mu_{\mathrm{Tot}} p_{2\mu} = 0,$$

$$\mathcal{M}_{\mathrm{Tot}} = \sum_{\text{all tri}} \mathcal{M}_{\mathrm{tri}} + \sum_{\text{all con}} \mathcal{M}_{\mathrm{con}}.$$

$$\Gamma = \frac{1}{2J+1} \frac{|\vec{p}|}{8\pi m_\psi^2} |\mathcal{M}^{\mathrm{Total}}|^2,$$

The widths of chosen processes

- In this work, we take the cut-off parameter α in the range $1.5 - 2$
- The coupling constants are obtained from our QPC calculation
- $\chi_{c3}(1F)$ production has a branching ratio on the order of 10^{-5}, and the $\chi_{c2}(1F)$ state exhibits a branching ratio around 10^{-4}
- The $\eta_{c2}(2D)$ state has an exceptionally small branching ratio $\sim 10^{-9}$, suppressed by heavy-quark spin symmetry
- The 1^3F_4 state is excluded from our study because its high angular momentum strongly suppresses its production

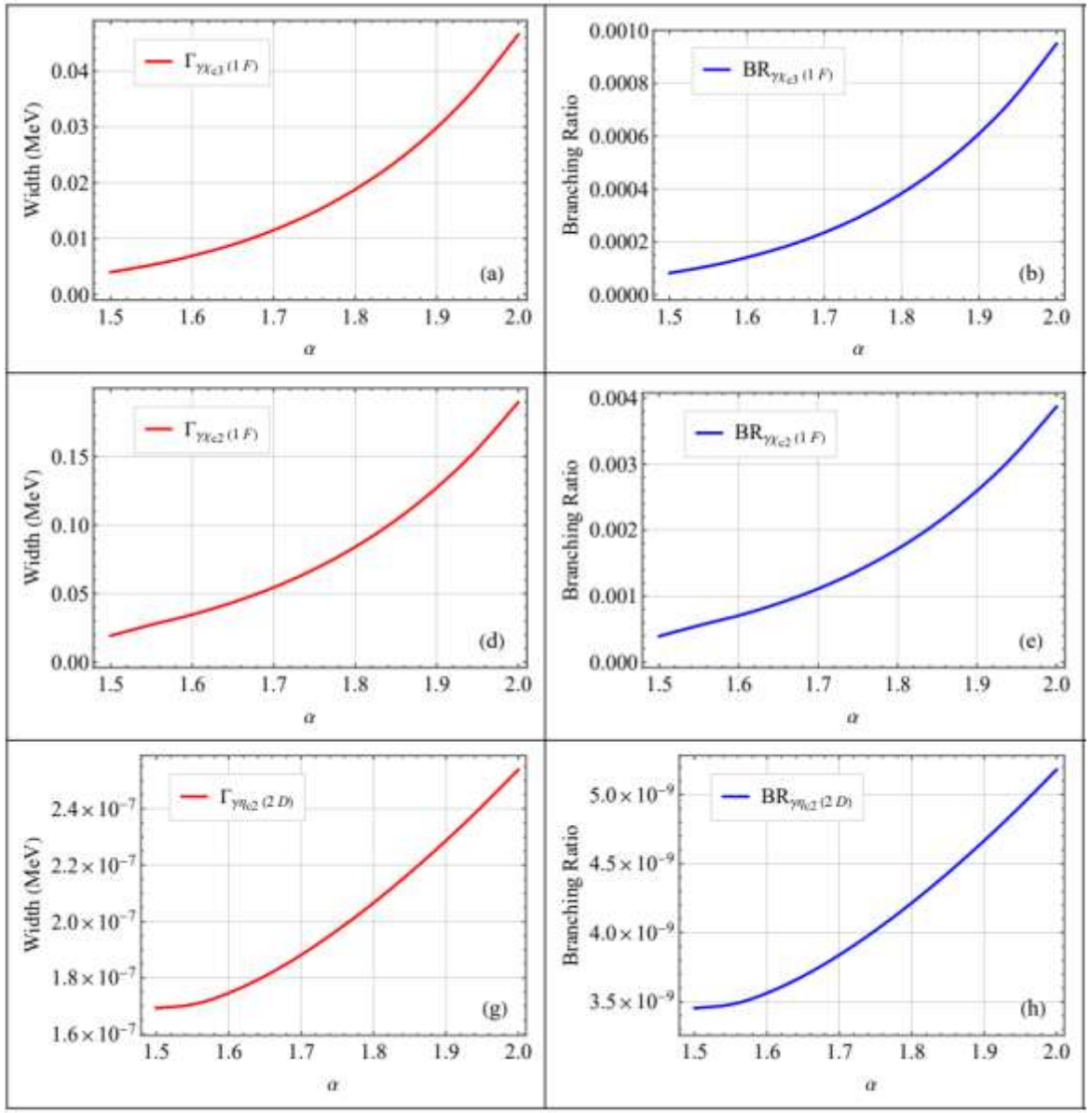

The production cross sections

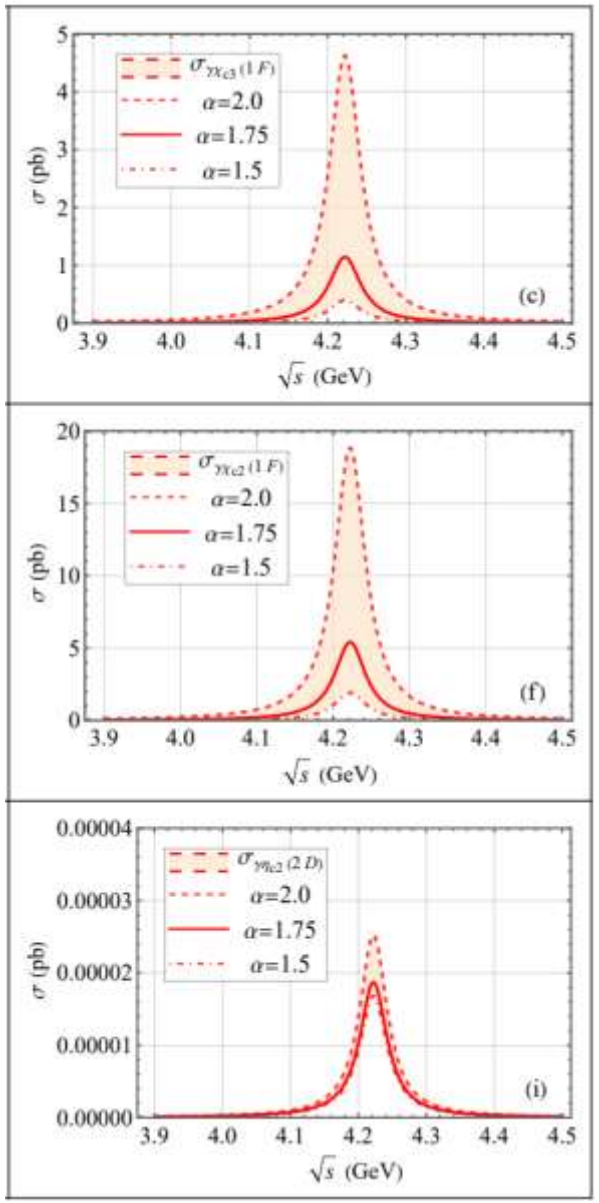

We are able to calculate their scattering cross section σ

$$\sigma(e^+e^- \to \psi(4230) \to \gamma X) = \frac{12\pi\Gamma_\psi^{e^+e^-}\Gamma_\psi^{\gamma X}}{|s - m_\psi^2 + im_\psi\Gamma_\psi|^2},$$

To quantify the model dependence, we presented the results for three typical values: $\alpha = 1.5, 1.75$, and 2

- $\sigma(\gamma\chi_{c3}(1F))$ is suppressed due to D-wave production and varies from approximately 0.5 pb to 5 pb, within the reach of next-generation experiments
- $\sigma(\gamma\chi_{c2}(1F))$ varies from about 2 pb to 20 pb. Searching for the $\chi_{c2}(1F)$ state via $e^+e^- \to \psi(4230) \to \gamma\chi_{c2}(1F)$ appears to be a promising avenue
- $\sigma(\gamma\eta_{c2}(2D)) \sim 2 \times 10^{-5}$ pb, showing negligible variation over the chosen range of α. Therefore, the discovery of the $\eta_{c2}(2D)$ likely relies on alternative production mechanisms

Summary

1. Recent observations of charmonia above 4 GeV motivate this investigation into high-lying states.

2. We perform a comprehensive study including mass spectrum (MGI model), two-body strong decays (QPC model), and radiative decays.

3. Production via e^+e^- annihilation is calculated, revealing promising search channels.

4. With upcoming facility upgrades, our results offer valuable guidance for experiments at BESIII, Belle II, and LHCb.

THANKS!